Original article

Folia Neuropathologica

Abnormalities in the normal appearing white matter of the cerebral hemisphere contralateral to a malignant brain tumor detected by diffusion tensor imaging

Kai Kallenberg[1], Torben Goldmann[1,2], Jan Menke[3], Herwig Strik[4], Hans C. Bock[5], Alexander Mohr[1], Jan H. Buhk[6], Jens Frahm[7], Peter Dechent[8], Michael Knauth[1]

[1]Institute for Diagnostic and Interventional Neuroradiology, Georg-August University, Göttingen, [2]MR-Research in Neurology and Psychiatry, Georg-August University, Göttingen, [3]Institute for Diagnostic and Interventional Radiology, Georg-August University, Göttingen, [4]Department of Neurology, University Medical Center, Philipps University, Marburg, [5]Department of Neurosurgery, Georg-August University, Göttingen, [6]Department of Neuroradiology, University Medical Center Hamburg-Eppendorf, Hamburg, [7]Biomedizinische NMR Forschungs GmbH, Göttingen, [8]MR-Research in Neurology and Psychiatry, Department of Cognitive Neurology, Georg-August University, Göttingen, Germany

Folia Neuropathol 2014; 52 (3): 226-233 DOI: 10.5114/fn.2014.45563

Abstract

Introduction: *Malignant brain tumors tend to migration and invasion of surrounding brain tissue. Histopathological studies reported malignant cells in macroscopically unsuspicious parenchyma (normal appearing white matter – NAWM) remote from the tumor localization. In early stages, diffuse interneural infiltration with changes of the apparent diffusion coefficient (ADC) and fractional anisotropy (FA) is hypothesized.*

Material and methods: *Patients' ADC and FA values from NAWM of the hemisphere contralateral to a malignant glioma were compared to age- and sex-matched normal controls.*

Results: *Apparent diffusion coefficient levels of the entire contralateral hemisphere revealed a significant increase and a decrease of FA levels. An even more pronounced ADC increase was found in a region mirroring the glioma location.*

Conclusions: *In patients with previously untreated anaplastic astrocytoma or glioblastoma, an increase of the ADC and a reduction of FA were found in the brain parenchyma of the hemisphere contralateral to the tumor localization. In the absence of visible MRI abnormalities, this may be an early indicator of microstructural changes of the NAWM attributed to malignant brain tumor.*

Key words: *glioma, normal appearing white matter, diffusion tensor imaging.*

Introduction

Magnetic resonance imaging (MRI) plays a central role in the treatment algorithms of patients with brain tumors. While conventional MRI with T2, FLAIR, and contrast-enhanced T1-weighted sequences unravel the size, shape, and structure of lesions, the use of perfusion- and diffusion-weighted MRI adds information about the regional blood volume and microstructural architecture. Additionally, pro-

Communicating author:
Dr. Kai Kallenberg, Institut für Diagnostische und Interventionelle Neuroradiologie, Universitätsmedizin Göttingen, Postfach, 37099 Göttingen, Germany, e-mail: kai.kallenberg@med.uni-goettingen.de

ton MR spectroscopy (MRS) gives insights into tissue composition and intracellular metabolism [15]. However, the technical progress in glioma imaging techniques seems to be ahead of the therapeutic achievements – initial promising results of local chemotherapy were overshadowed by reports of wound healing disorders and even deaths [9] and the lack of long-term effects. Probably, microinvasive expansion is the main reason why malignant brain tumors still cannot be cured with local treatment such as surgery, focal irradiation or local chemotherapy [10]. Several studies have reported the infiltrative growth of glioblastoma multiforme (GBM) cells in apparently unaffected brain regions remote from the confirmed primary lesion [5,17,24,32] without correlating changes on computed tomographic or MR images [20,38]. Diffusion tensor imaging (DTI) [2,14,34] and localized proton MRS provided subtle hints towards remote infiltration of GBM cells [4,14,18]. This work investigated the use of DTI and corresponding metrics as putative indicators of the invasiveness of malignant brain tumors.

Material and methods

The local ethics committee approved this work according to the Declaration of Helsinki. Written informed consent was obtained from all patients and control subjects. Prospectively, over a time period of 2 years pre-operative DTI was performed in all cases of suspected brain tumor. Only patients with newly diagnosed and post-operative definite histopathological confirmation of malignant brain tumor (astrocytoma WHO grade III or glioblastoma WHO grade IV) were included if there was no history of previous malignancies. Healthy age- and sex-matched volunteers without any relevant medical history, especially tumor or systemic chemotherapy, served as normal controls – patients and volunteers were matched on an individual basis. Data analyses were performed retrospectively.

Two neuroradiologists blinded to the study (J.H.B., A.M.) reviewed the clinical MR images and ruled out MRI evidence of tumor infiltration of the hemisphere contralateral to the tumor or other pathologies (e.g. malformations, enlarged perivascular spaces, calcifications or blood remnants). The standard clinical MRI protocol comprised T2, FLAIR, DWI, and T1 sequences without and with contrast agent. An extra set of T2w and PDw images was acquired from the volunteers to rule out relevant abnormalities. Minor unspecific or microvascular signal alterations of the white matter usually referred to as "age related" (Fazekas scale grade 1 [8]) were present in some patients and controls as well and were not excluded if there was no history of related symptoms and if the lesions did not exceed an estimated 10% of the complete ROI.

Magnetic resonance imaging

All examinations were performed on the same 3 Tesla-MR system (Magnetom Trio, Siemens, Erlangen/Germany). Anatomical imaging included T1-weighted three-dimensional fast low-angle shot (FLASH) sequence (time-to-repetition TR 11 ms; time-to-echo TE 4.9 ms; flip angle 15°; isotropic image resolution $1 \times 1 \times 1$ mm^3). Diffusion tensor imaging employed single-shot stimulated echo acquisition mode (STEAM) MRI without diffusion gradients and with 24 different diffusion gradient directions (b-value 1000 s/mm^2, 38 axial sections, 3 acquisitions) at $2.2 \times 2.2 \times 2.2$ mm^3 image resolution. For further details see [28].

STEAM MRI acquisition is negligibly sensitive to magnetic field inhomogeneity, so the undistorted STEAM images as well as the resulting fractional anisotropy (FA) maps and apparent diffusion coefficient (ADC) maps are spatially congruent to the anatomical images. Without the need for a co-registration or alignment technique, which is usually accompanied by a certain degree of blurring, the present work allowed for a direct digital superposition of corresponding data matrices [13]. After preprocessing applying a Neeman correction [25] region-of-interest (ROI) measurements were performed on FA and ADC maps applying the dedicated software package *effective Diffusion Coefficient Navigator* (DeffCoN, for details see [23]) [3,6,12,13]. Each ROI was manually defined first on the anatomic images (Fig. 1) and subsequently confirmed on FA and ADC maps: The ROI "Hemisphere$_C$" refers to the normal appearing white matter (NAWM) of the cerebral hemisphere contralateral to the tumor 2 mm cranial to the lateral ventricle preventing partial volume artifacts. The ROI "ROI$_C$" denotes only the white matter in the contralateral hemisphere in an area mirroring the tumor site on the section with the largest tumor extends. ROI$_C$ was manually drawn to ensure confinement to white matter, since a simple mirror of the tumor would have included grey matter and/or CSF. In addition, the data from the tumor

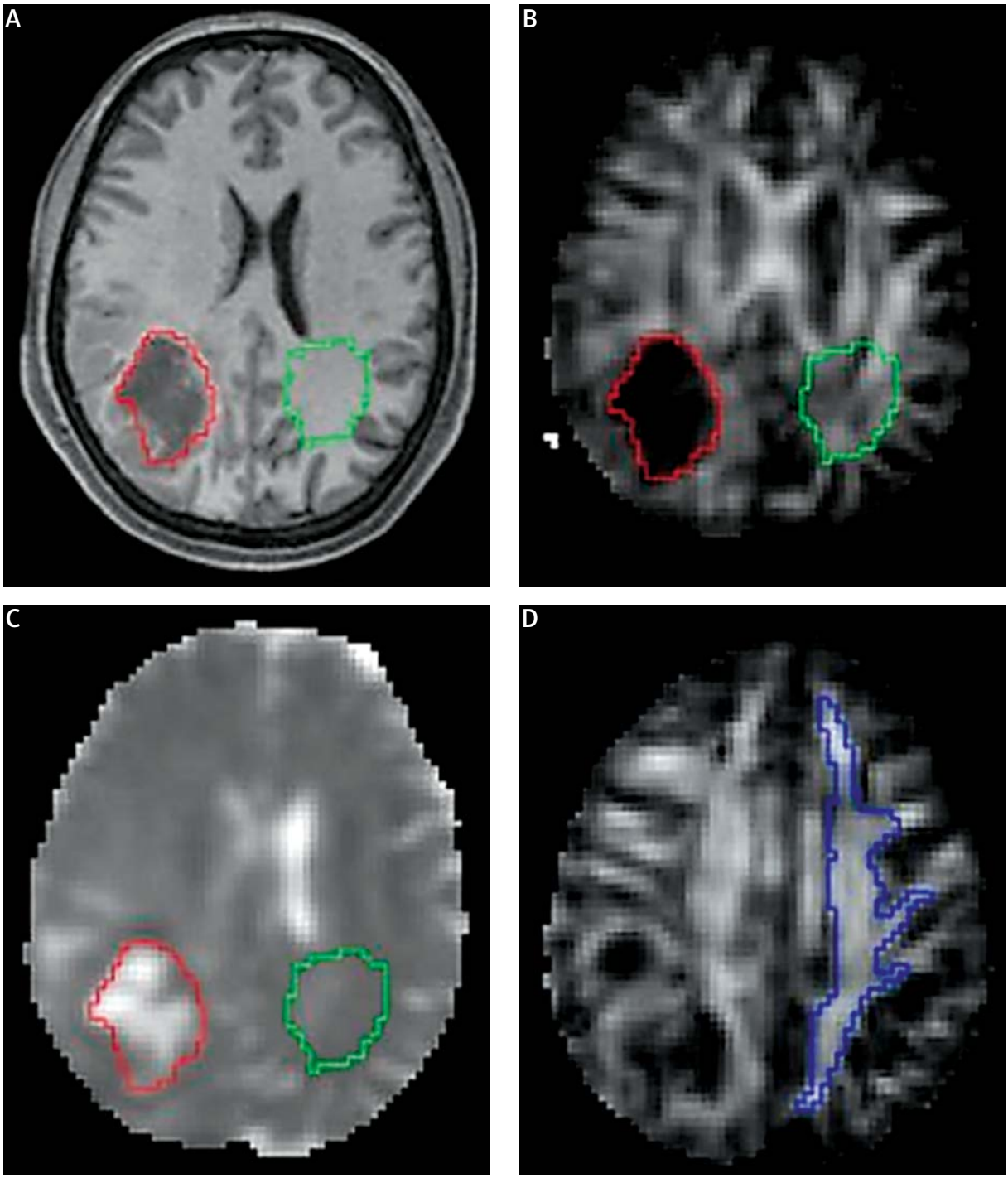

Fig. 1. A) Axial section of the 3D T1-weighted data set, **B)** FA map, **C)** ADC map, **D)** FA map 2 mm cranial of the left ventricle. The tumor is surrounded by a red line. A green line defines the ROI_C in the contralateral hemisphere mirroring the tumor; the blue line defines the $Hemisphere_C$ in the white matter of the contralateral hemisphere (**D**).

location (ROI of "tumor") were acquired in a similar manner. The control ROIs were placed in both hemispheres of the age- and sex-matched controls in the same anatomical location as the patients' ROIs. Then the mean of both control ROIs was compared to the patients' data. Distinct emphasis was put on

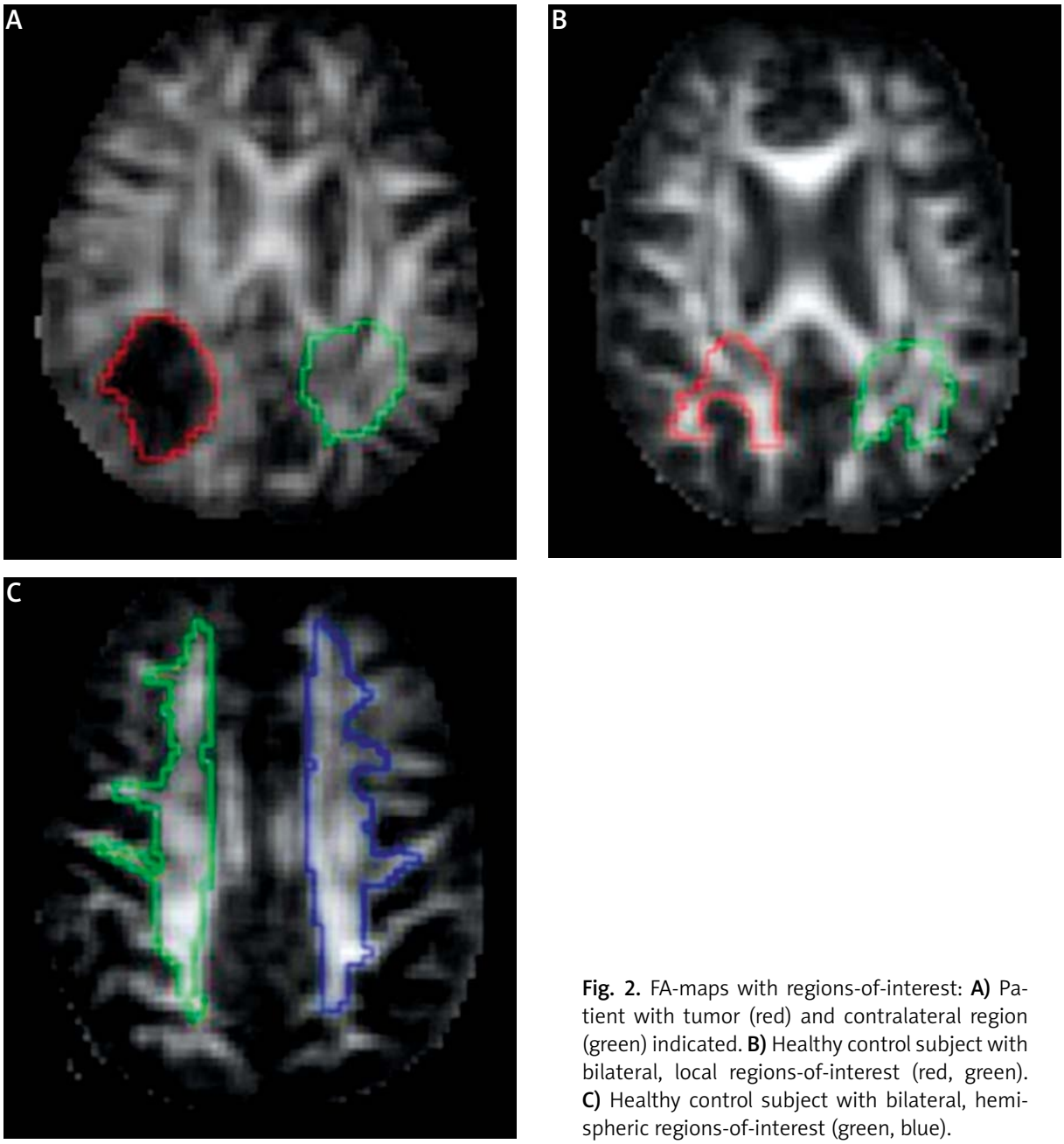

Fig. 2. FA-maps with regions-of-interest: **A)** Patient with tumor (red) and contralateral region (green) indicated. **B)** Healthy control subject with bilateral, local regions-of-interest (red, green). **C)** Healthy control subject with bilateral, hemispheric regions-of-interest (green, blue).

preventing partial volume effects, so that in cases of uncertainty the ROI was diminished and safety margins were considered. Differences in brain size or white matter volume resulted in minor ROI volume differences. The positioning was performed (T.G.) after adequate training and under supervision of an experienced neuroradiologist (K.K.). The person positioning the ROI and the supervising neuroradiologist were aware of the purpose of the study.

Statistical analyses

ADC and FA values of the patient group and the matched control group were compared using unpaired Student's *t*-tests. Additionally, intra-individual differences between the study parameters ROI_C vs. $Hemisphere_C$ were analyzed by paired *t*-tests, both for the patient group and the control group. The significance level was generally set to $p < 0.05$.

Results

Fifty-two patients were scanned according to the MRI protocol. Sixteen did not match the inclusion criteria and had to be excluded (3 patients with lymphoma, 6 with metastasis and 7 with low-grade tumors: 5 WHO II, 2 WHO I). One patient with tumor spread into the contralateral hemisphere was also excluded. One patient terminated the examination intentionally and 3 had to be excluded because of motion artifacts.

The analysis comprised 31 patients who completed the MRI scan and fulfilled the inclusion criteria: 13 females, 18 males; mean age 56.9 years (22-77 years). The post-operative neuropathological diagnosis was astrocytoma WHO grade III in 8 cases and glioblastoma multiforme WHO grade IV in 23 cases. DTI datasets of 31 healthy age- and sex-matched volunteers served as the control (mean age 57.3 years [23-81 years]).

The FA values were significantly lower in the NAWM ($Hemisphere_C$) of the tumor patients compared to controls ($p < 0.01$). Accordingly, the ADC values for NAWM in the contralateral hemisphere were elevated ($p < 0.01$). This finding was particularly pronounced in the area ROI_C mirroring the obvious tumor localization (Table I).

In the healthy controls the study parameters $Hemisphere_C$ and ROI_C showed no significant intra-individual differences (Table II), and the same applied for the FA values in the tumor patients ($p = 0.55$). However, in the tumor patients the ADC values of ROI_C were significantly higher compared to the ADC values of $Hemisphere_C$ ($p < 0.01$).

Discussion

Glioma cells initially infiltrate or spread microinvasively between and around neurons and pene-

Table I. Comparison of patients versus controls

Study parameter	Patients	Controls	Difference$	*p*-value*
	Mean (SD)	Mean (SD)	Mean (SD)	
Age (years)	56.9 (14.2)	57.3 (13.9)	–0.3 (7.1)	0.91
FA of ipsilateral tumor location#	0.077 (0.034)	0.285 (0.033)	–0.208 (0.017)	**< 0.01**
FA of contralateral ROI_C§	0.253 (0.040)	0.285 (0.033)	–0.033 (0.019)	**< 0.01**
FA of contralateral $Hemisphere_C$&	0.258 (0.028)	0.283 (0.018)	–0.025 (0.012)	**< 0.01**
ADC of ipsilateral tumor location#	1.357 (0.365)	0.724 (0.053)	0.632 (0.132)	**< 0.01**
ADC of contralateral ROI_C§	0.793 (0.093)	0.724 (0.053)	0.068 (0.038)	**< 0.01**
ADC of contralateral $Hemisphere_C$&	0.735 (0.045)	0.706 (0.035)	0.029 (0.020)	**< 0.01**

ADC – apparent diffusion coefficient (in units of 10^{-3} mm^2/s), FA – fractional anisotropy
*$ – mean difference of the patient group minus the control group, * – the patient and control groups were compared by unpaired t-tests, with significant differences (p < 0.05) printed in bold, & – $Hemisphere_C$ refers to the normal appearing white matter (NAWM) of the cerebral hemisphere contralateral to the tumor, 2 mm cranial to the lateral ventricle, § – ROI_C denotes only the white matter in the contralateral hemisphere in an area mirroring the tumor site on the slide with the largest tumor extent, # – in each patient the "tumor location" was mirrored to a similar anatomical region in the corresponding matched control*

Table II. Intra-individual comparison of $Hemisphere_C$ versus ROI_C

Study parameter	$Hemisphere_C$&	ROI_C§	Difference$	*p*-value*
	Mean (SD)	Mean (SD)	Mean (SD)	
FA in patients#	0.258 (0.028)	0.253 (0.040)	0.005 (0.016)	0.55
ADC in patients#	0.735 (0.045)	0.793 (0.093)	–0.058 (0.034)	**< 0.01**
FA in controls§	0.283 (0.018)	0.285 (0.033)	–0.003 (0.014)	0.70
ADC in controls§	0.706 (0.035)	0.724 (0.053)	–0.018 (0.019)	0.07

ADC – apparent diffusion coefficient (in units of 10^{-3} mm^2/s), FA – fractional anisotropy
*& – $Hemisphere_C$ refers to the normal appearing white matter (NAWM) of the cerebral hemisphere contralateral to the tumor, 2 mm cranial to the lateral ventricle, § – ROI_C denotes only the white matter in the contralateral hemisphere in an area mirroring the tumor site on the slide with the largest tumor extent, $ – mean difference of both study parameters ($Hemisphere_C$ minus ROI_C), * – the study parameters $Hemisphere_C$ versus ROI_C were compared by paired t-tests, with significant values (p < 0.05) printed in bold*

trate into the fiber tracts of the white matter. In early stages, tumor infiltration leads to increased cellularity without destruction of neurons, and to neovascularization [29]. Diffusion tensor imaging metrics are sensitive to changes of fiber tract architecture on a microscopic level [26,34]. Glioma cells in the early invasion stages cause local displacement of parenchyma without neuronal damage [26], resulting in increased ADC values analogous to the characteristics of low-grade gliomas [7]. In an animal model lower FA and higher perpendicular diffusivity were demonstrated in the infiltration zone of a glioblastoma xenograft compared to normal white matter of the same animal [37]. Inglese *et al.* found an increase of the ADC in the contralateral cerebral hemisphere of glioma patients [14]. A negative correlation of cell number and percentage of tumor infiltration with FA was reported by other groups [30,33]. Accordingly, a low FA value in the hemisphere contralateral to the tumor, as found in the present work, is compatible with early stages of tumor infiltration. In the further course of disease, nerve cells may be destroyed and replaced by tumor cells [29], resulting in an ADC decrease [11] and an FA increase [1]. The latter finding might not be expected to be a specific sign of early tumor formation, because the FA is regarded as an unspecific parameter for fiber tract integrity. However, there is a certain order in tumor cell architecture of vital glioblastoma tissue that causes an increase of FA and kurtosis [27,37].

Glioma cell invasion depends on destruction of extracellular matrix components as well as on penetration between adjacent normal brain structures [35]. This causes an increase in diffusivity and thus facilitates an increase of the ADC value. Furthermore, the growth of a tumor in the CNS is associated with a disturbance of the blood-brain barrier, which leads to a vasogenic edema and an increase in parenchymal water content, which in turn increases the extracellular space and the tissue ADC value [21].

In the present study, in the tumor patients increased ADC values were more pronounced in the parenchyma mirroring the tumor area (ROI_C) than in the entire contralateral hemisphere ($Hemisphere_C$). The corresponding FA differences were not significant. The ADC diffusion values underscore a mainly local effect and so make a uniform global brain edema improbable. The observed constellation may therefore be interpreted as infiltrating malignant cells at the time of MRI, in concordance with the previously described invasion pattern of malignant glioma cells along the fiber tracts of white matter [16]. The more pronounced ADC changes in ROI_C suggest a preference of tumor spread to the corresponding mirrored contralateral brain parenchyma before expanding into the entire contralateral hemisphere ($Hemisphere_C$). A possible explanation would be spreading along the commissural tracts. This is in line with previous DTI studies [19,22] and the observation that remote tumor cells histopathologically match the primary glioma [32].

Abnormal FA or ADC values are not a proof of malignant transformation as they cannot differentiate between tumor and edema [31]. Apparent diffusion coefficient may be influenced by several parameters such as cellular density, existence and distribution of vasogenic edema, and tissue hypoxia [11]. The results in this study may, to some extent, also be attributed to diaschisis, which refers to metabolic and functional changes remote from the origin but communicating with the damaged focus via anatomical structures [36]. However, previous MRS findings in normal appearing white matter in tumor patients indicate the presence of proliferative processes [18].

The present results add further evidence of alterations of normal appearing brain parenchyma in the cerebral hemisphere contralateral to a malignant brain tumor. In the context of previous histopathological studies this effect may be interpreted as an indication of malignant cells. In the present study, however, no neuropathological data were collected to prove this hypothesis.

Conclusion

In patients with previously untreated anaplastic astrocytoma or glioblastoma, an increase of the apparent diffusion coefficient (ADC) and a reduction of fractional anisotropy (FA) were found in the brain parenchyma of the hemisphere contralateral to the tumor localization. In the absence of visible MRI abnormalities, this may be an early indicator of microstructural changes of the NAWM attributed to malignant brain tumor.

Disclosure

The authors (K.K., J.H.B. and P.D.) were supported by the Volkswagen Stiftung (Grants ZN1635 and ZN 2193).

Authors report no conflict of interest.

References

1. Beppu T, Inoue T, Shibata Y, Yamada N, Kurose A, Ogasawara K, Ogawa A, Kabasawa H. Fractional anisotropy value by diffusion tensor magnetic resonance imaging as a predictor of cell density and proliferation activity of glioblastomas. Surg Neurol 2005; 63: 56-61.
2. Bobek-Billewicz B, Stasik-Pres G, Majchrzak K, Senczenko W, Majchrzak H, Jurkowski M, Poletek J. Fibre integrity and diffusivity of the pyramidal tract and motor cortex within and adjacent to brain tumour in patients with or without neurological deficits. Folia Neuropathol 2011; 49: 262-270.
3. Boretius S, Michaelis T, Tammer R, Ashery-Padan R, Frahm J, Stoykova A. In vivo MRI of altered brain anatomy and fiber connectivity in adult pax6 deficient mice. Cereb Cortex 2009; 19: 2838-2847.
4. Busch M, Liebenrodt K, Gottfried S, Weiland E, Vollmann W, Mateiescu S, Winter S, Lange S, Sahinbas H, Baier J, van Leeuwen P, Gronemeyer D. Influence of brain tumors on the MR spectra of healthy brain tissue. Magn Reson Med 2011; 65: 18-27.
5. de Bouard S, Christov C, Guillamo JS, Kassar-Duchossoy L, Palfi S, Leguerinel C, Masset M, Cohen-Hagenauer O, Peschanski M, Lefrancois T. Invasion of human glioma biopsy specimens in cultures of rodent brain slices: a quantitative analysis. J Neurosurg 2002; 97: 169-176.
6. Dreha-Kulaczewski SF, Helms G, Dechent P, Hofer S, Gartner J, Frahm J. Serial proton MR spectroscopy and diffusion tensor imaging in infantile Balo's concentric sclerosis. Neuroradiology 2009; 51: 113-121.
7. Essig M, Giesel F, Stieltjes B, Weber MA. Functional imaging for brain tumors (perfusion, DTI and MR spectroscopy). Radiologe 2007; 47: 513-519 [in German].
8. Fazekas F, Chawluk JB, Alavi A, Hurtig HI, Zimmerman RA. MR signal abnormalities at 1.5 T in Alzheimer's dementia and normal aging. AJR Am J Roentgenol 1987; 149: 351-356.
9. Gallego JM, Barcia JA, Barcia-Marino C. Fatal outcome related to carmustine implants in glioblastoma multiforme. Acta Neurochir (Wien) 2007; 149: 261-265.
10. Giese A, Bjerkvig R, Berens ME, Westphal M. Cost of migration: invasion of malignant gliomas and implications for treatment. J Clin Oncol 2003; 21: 1624-1636.
11. Hartmann M, Junkers R, Herold-Mende C, Ahmadi R, Heiland S. Pseudonormalization of diffusion weighted images: magnetic resonance imaging in an animal model (C6-glioma). Rofo 2005; 177: 114-118 [in German].
12. Hofer S, Frahm J. Topography of the human corpus callosum revisited – comprehensive fiber tractography using diffusion tensor magnetic resonance imaging. Neuroimage 2006; 32: 989-994.
13. Hofer S, Karaus A, Frahm J. Reconstruction and dissection of the entire human visual pathway using diffusion tensor MRI. Front Neuroanat 2010; 4: 15.
14. Inglese M, Brown S, Johnson G, Law M, Knopp E, Gonen O. Whole-brain N-acetylaspartate spectroscopy and diffusion tensor imaging in patients with newly diagnosed gliomas: a preliminary study. AJNR Am J Neuroradiol 2006; 27: 2137-2140.
15. Jaskolski DJ, Fortuniak J, Majos A, Gajewicz W, Papierz W, Liberski PP, Sikorska B, Stefanczyk L. Magnetic resonance spectroscopy in intracranial tumours of glial origin. Neurol Neurochir Pol 2013; 47: 438-449.
16. Johnson PC, Hunt SJ, Drayer BP. Human cerebral gliomas: correlation of postmortem MR imaging and neuropathologic findings. Radiology 1989; 170: 211-217.
17. Kageji T, Nagahiro S, Uyama S, Mizobuchi Y, Toi H, Nakamura M, Nakagawa Y. Histopathological findings in autopsied glioblastoma patients treated by mixed neutron beam BNCT. J Neurooncol 2004; 68: 25-32.
18. Kallenberg K, Bock HC, Helms G, Jung K, Wrede A, Buhk JH, Giese A, Frahm J, Strik H, Dechent P, Knauth M. Untreated glioblastoma multiforme: increased myo-inositol and glutamine levels in the contralateral cerebral hemisphere at proton MR spectroscopy. Radiology 2009; 253: 805-812.
19. Kallenberg K, Goldmann T, Menke J, Strik H, Bock HC, Stockhammer F, Buhk JH, Frahm J, Dechent P, Knauth M. Glioma infiltration of the corpus callosum: early signs detected by DTI. J Neurooncol 2013; 112: 217-222.
20. Kelly PJ, Daumas-Duport C, Kispert DB, Kall BA, Scheithauer BW, Illig JJ. Imaging-based stereotaxic serial biopsies in untreated intracranial glial neoplasms. J Neurosurg 1987; 66: 865-874.
21. Kono K, Inoue Y, Nakayama K, Shakudo M, Morino M, Ohata K, Wakasa K, Yamada R. The role of diffusion-weighted imaging in patients with brain tumors. AJNR Am J Neuroradiol 2001; 22: 1081-1088.
22. Krishnan AP, Asher IM, Davis D, Okunieff P, O'Dell WG. Evidence that MR diffusion tensor imaging (tractography) predicts the natural history of regional progression in patients irradiated conformally for primary brain tumors. Int J Radiat Oncol Biol Phys 2008; 71: 1553-1562.
23. Küntzel M. Parallele Datenakquisition zur Beschleunigung diffusions-gewichteter Kernspintomographie mit stimulierten Echos. Göttingen Georg-August-Universität, 2007.
24. Matsukado Y, Maccarty CS, Kernohan JW. The growth of glioblastoma multiforme (astrocytomas, grades 3 and 4) in neurosurgical practice. J Neurosurg 1961; 18: 636-644.
25. Neeman M, Freyer JP, Sillerud LO. A simple method for obtaining cross-term-free images for diffusion anisotropy studies in NMR microimaging. Magn Reson Med 1991; 21: 138-143.
26. Price SJ, Burnet NG, Donovan T, Green HA, Pena A, Antoun NM, Pickard JD, Carpenter TA, Gillard JH. Diffusion tensor imaging of brain tumours at 3T: a potential tool for assessing white matter tract invasion? Clin Radiol 2003; 58: 455-462.
27. Raab P, Hattingen E, Franz K, Zanella FE, Lanfermann H. Cerebral gliomas: diffusional kurtosis imaging analysis of microstructural differences. Radiology 2010; 254: 876-881.
28. Rieseberg S, Merboldt KD, Kuntzel M, Frahm J. Diffusion tensor imaging using partial Fourier STEAM MRI with projection onto convex subsets reconstruction. Magn Reson Med 2005; 54: 486-490.
29. Scherer HJ. Structural development in gliomas. Am J Cancer 1938; 34: 333-351.
30. Schluter M, Stieltjes B, Hahn HK, Rexilius J, Konrad-Verse O, Peitgen HO. Detection of tumour infiltration in axonal fibre

bundles using diffusion tensor imaging. Int J Med Robot 2005; 1: 80-86.
31. Server A, Kulle B, Maehlen J, Josefsen R, Schellhorn T, Kumar T, Langberg CW, Nakstad PH. Quantitative apparent diffusion coefficients in the characterization of brain tumors and associated peritumoral edema. Acta Radiol 2009; 50: 682-689.
32. Silbergeld DL, Chicoine MR. Isolation and characterization of human malignant glioma cells from histologically normal brain. J Neurosurg 1997; 86: 525-531.
33. Stadlbauer A, Ganslandt O, Buslei R, Hammen T, Gruber S, Moser E, Buchfelder M, Salomonowitz E, Nimsky C. Gliomas: histopathologic evaluation of changes in directionality and magnitude of water diffusion at diffusion-tensor MR imaging. Radiology 2006; 240: 803-810.
34. Stieltjes B, Schluter M, Didinger B, Weber MA, Hahn HK, Parzer P, Rexilius J, Konrad-Verse O, Peitgen HO, Essig M. Diffusion tensor imaging in primary brain tumors: reproducible quantitative analysis of corpus callosum infiltration and contralateral involvement using a probabilistic mixture model. Neuroimage 2006; 31: 531-542.
35. Tysnes BB, Mahesparan R. Biological mechanisms of glioma invasion and potential therapeutic targets. J Neurooncol 2001; 53: 129-147.
36. von Monakow C. Die Lokalisation im Grosshirn und der Abbau der Funktion durch kortikale Herde. J.F. Bergmann, Wiesbaden 1914, p. 1033.
37. Wang S, Zhou J. Diffusion tensor magnetic resonance imaging of rat glioma models: a correlation study of MR imaging and histology. J Comput Assist Tomogr 2012; 36: 739-744.
38. Watanabe M, Tanaka R, Takeda N. Magnetic-resonance-imaging and histopathology of cerebral gliomas. Neuroradiology 1992; 34: 463-469.